J Infrared Milli Terahz Waves (2025) 46:12
https://doi.org/10.1007/s10762-024-01027-3

RESEARCH

High-Isolation Array Antenna Design for 5G mm-Wave MIMO Applications

Nisar Ahmad Abbasi[1] · Bal Virdee[2] · Iftikhar Ud Din[3] · Sadiq Ullah[3] · Ayman A. Althuwayb[4] · Nasr Rashid[4,5] · Mohammad Soruri[6] · Chan Hwang See[7] · Mohammad Alibakhshikenari[8]

Received: 30 June 2024 / Accepted: 24 November 2024

Abstract
A low form-factor design of an eight-element antenna array is presented for 5G mm-wave MIMO applications. The design features modified circular patch radiators that achieve an impedance bandwidth of 2.6 GHz, covering frequencies from 37.7 to 40.3 GHz. The radiating elements are strategically arranged on opposite sides of a common substrate and interleaved to significantly reduce mutual coupling between adjacent elements. This innovative technique effectively minimizes coupling between the array's radiators without the need of a decoupling structure. The MIMO antenna is fabricated on a low-loss Rogers-5880 substrate, with a thickness of 0.8 mm, a dielectric constant of 2.2, and a loss tangent of 0.0009, ensuring minimal signal loss and confirming the accuracy of simulation results. The inter-element isolation exceeds 25 dB, and the array provides a gain greater than 6 dBi, with a peak gain of 7.5 dBi at 39 GHz. This high gain enhances the antenna's ability to mitigate atmospheric attenuation at higher frequencies, making it highly suitable for 5G mm-wave applications.

Keywords Millimeter wave (mmWave) · Antenna array · MIMO antennas · High isolation · 5G communications

1 Introduction

The recent times have seen a rapid advancement. Recent advancements in mobile communication have driven a growing demand for increased capacity and wider bandwidth. Fifth-generation (5G) technology addresses this demand by offering a transmission capacity of up to 20 Gbps and ultra-low latency of 1 ms, facilitating a range of applications such as virtual reality, autonomous vehicles, and smart cities [1, 2]. In addition to improving connectivity for millions of devices, 5G also enhances network reliability and performance [3, 4].

Extended author information available on the last page of the article

Published online: 21 December 2024

Many leading countries are leveraging the millimeter-wave (mmWave) spectrum for 5G wireless communication [5–7]. With increasing congestion and reduced capacity in the sub-6 GHz frequency range, mmWave technology offers a viable solution by providing greater bandwidth for 5G networks. The advantages of mmWave technology include higher data rates, broader bandwidth, enhanced security, and reduced susceptibility to multipath fading, making it an attractive option for next-generation mobile communication systems [8, 9].

However, mmWave signals face challenges, particularly high path loss, which limits their communication range during propagation. The design of mmWave antennas differs significantly from those operating in the sub-6 GHz range, particularly in terms of geometry for mobile station setups [10].

Several mmWave planar waveguide-based array antennas with wide bandwidth and high gain have been reported in the literature [11, 12]. Array antennas often rely on network feeding techniques to distribute input power among the radiating elements, with two commonly used approaches being series-fed network arrays and parallel-fed network arrays [13]. While both approaches exhibit good radiation characteristics, parallel-fed arrays tend to have more complex designs and larger dimensions [14]. In contrast, series-fed networks suffer from limited impedance bandwidth as the number of radiating elements increases [15].

A promising solution to these challenges is MIMO (Multiple Input Multiple Output) technology, which addresses the limitations of a single radiating element in wireless communication [16]. In a MIMO system, identical radiating elements are duplicated across the same plane, operating at the same frequency range, allowing the configuration to be easily modified. Spatial multiplexing, a key feature of MIMO, enhances channel capacity, leading to increased data rates, reduced multipath fading, high efficiency, wide bandwidth, and a high signal-to-noise ratio (SNR) [17].

Extensive research has been conducted on various antenna arrays for mmWave MIMO systems. For example, a two-element array operating at 28 GHz is presented in [18], offering strong isolation and a gain of 5.42 dB. A four-element array, operating at 27 GHz with dimensions of $30 \times 30 \times 1.575$ mm^3, is proposed in [19], achieving a peak gain of 7.1 dB and wide bandwidth. Another four-element array, operating in the 25.5–29.6 GHz range, is discussed in [20], with a maximum gain of 8.3 dB but lower isolation of 17 dB.

Further, [21] introduces a novel planar helix-inspired two-port array operating in the 28 GHz band, with a modest gain of 5.8 dB and strong isolation. In [22], a four-element array antenna designed for Ka-band mmWave applications is presented, featuring a peak gain of 6.1 dB and a perpendicular arrangement of the radiating elements on the substrate, offering good isolation.

Additionally, a DRA (Dielectric Resonator Antenna) 4×4 array is suggested for mmWave communication in [23], built on an FR-4 substrate with slotted ground and aperture-coupled feeding. This design achieves a bandwidth of 26.71 to 28.91 GHz, with a peak gain of 7 dB and isolation of 29 dB at 28 GHz. A four-element array with a defected ground structure to improve impedance bandwidth is proposed in [24]. This system, operating at 26.414 GHz, features a maximum gain of 7 dB.

In [25], a two-element array for 5G communication, operating at 28 GHz, is designed with elements placed parallel on the upper surface of the substrate. A metamaterial slab is introduced between the radiating elements to enhance radiation performance. Lastly, a broadband FSS-based UWB antenna covering 3–12 GHz is proposed in [26, 27]. The use of an FSS surface improves the antenna's gain at 9 GHz from 5 to 8.1 dB, although it increases the size and complexity of the design.

This article presents an eight-element antenna array designed for 5G mm-wave MIMO applications. The proposed antenna features wide bandwidth, high gain, and excellent MIMO performance, including low envelope correlation coefficient (ECC) and high diversity gain. The radiating element is based on a standard circular patch antenna, but its configuration has been modified to enhance radiation properties. Notably, the antenna achieves an exceptionally low reflection coefficient of − 50 dB at its resonant frequency, indicating minimal signal reflection and high radiation efficiency. Additionally, the design employs a strategic arrangement in which the radiating elements are positioned on opposite sides of the array and interleaved, significantly improving isolation and overall performance.

2 Antenna Array Configuration

2.1 Single Antenna Element

The radiating element constituting the antenna array is based on a circular patch. The initial step involves designing a circular patch antenna with a full ground plane. This configuration was chosen for its symmetrical radiation pattern and its wide impedance bandwidth. The radius of the circular patch can be calculated using [28]:

$$R = 8.79 \times 109/f_r\sqrt{\varepsilon_r}\left\{\frac{2h}{1+\pi\varepsilon_r F\left[ln\left(\frac{\pi F}{2h}\right)\right]+1.7726}\right\} \quad (1)$$

where f_r is the resonance frequency, h is the substrate height, ε_r is the diectric constant of the substrate, and v_o is the free space velocity of light.

To improve the antenna's radiation characteristics, semi-circular sections were strategically removed from the patch, as illustrated in Fig. 1. These modifications alter the current distribution over the patch, which in turn optimizes the antenna's performance. Notably, the changes result in a significantly enhanced impedance match, shown in Fig. 2, achieving a return loss of − 50 dB at the resonant frequency of 38.9 GHz. This excellent impedance match minimizes signal reflections, leading to high radiation efficiency. These results were obtained using CST Studio Suite which is a 3D electromagnetic (EM) analysis tool. The antenna was designed on a 0.8-mm thick, low-loss, high-frequency Rogers RT-5880 substrate with a relative permittivity (ε_r) of 2.2. Dimensions of the antenna's design parameters are listed in Table 1.

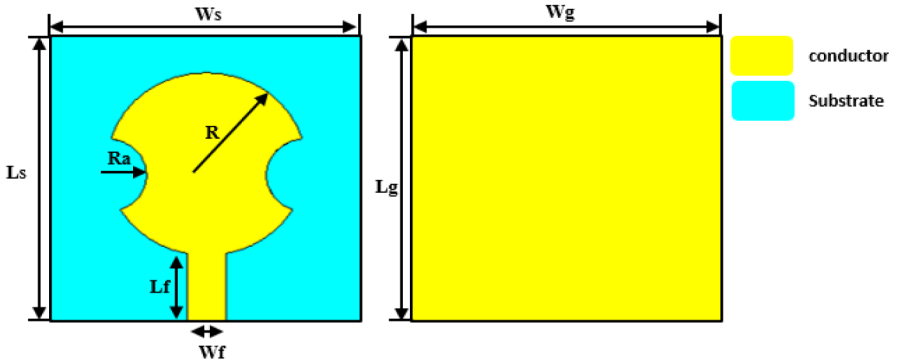

Fig. 1 Modified circular patch antenna; **a** front view and **b** back view

The antenna demonstrates a broad impedance bandwidth, with a reflection coefficient better than − 10 dB across a 2.6 GHz range, extending from 37.7 to 40.3 GHz. Over this bandwidth, the antenna achieves a stable gain of 4.91 dB, contributing to reliable signal transmission and reception. The wide bandwidth is particularly advantageous for supporting high data rates, which are essential for modern high-frequency communication systems. Additionally, the combination of a low reflection coefficient and high gain ensures that the antenna operates efficiently within the specified frequency range, making it suitable for applications requiring robust and high-performance operation in the millimeter-wave spectrum.

2.2 Effect of Modifying the Circular Antenna

The parametric study in Fig. 3 shows how the semi-circular section subtracted from the circular patch influences the reflection coefficient and gain of the proposed antenna. The key parameter influencing the antenna's performance is the radius of the semi-circular radius (Ra). Figure 3a shows that as the radius of the semi-circular cut (Ra) increases, the antenna's resonant frequency shifts higher, and the reflection coefficient improves for Ra values ranging from 0.1 to 1.5 mm. However, for radii greater than 1.5 mm, the reflection coefficient begins to deteriorate. In Fig. 3b, the gain is highest for an Ra of 0.1 mm in the frequency ranges between 35 and 36.5 GHz and between 39.5 and 45 GHz. The lowest gain is observed for an Ra of 0.8 mm. The impact of Ra on the antenna's performance is summarized in Table 2.

2.3 Two Element Array

The two radiating elements are positioned in close proximity to form a two-element array, as illustrated in Fig. 4. The gap between the antennas was carefully adjusted to 8 mm in order to minimize the detrimental effects of mutual coupling. The array was fabricated on a 0.8 mm thick Rogers RT-5880 substrate,

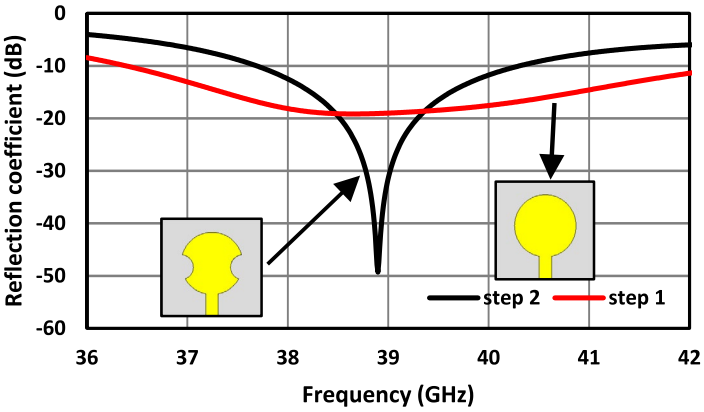

(a)

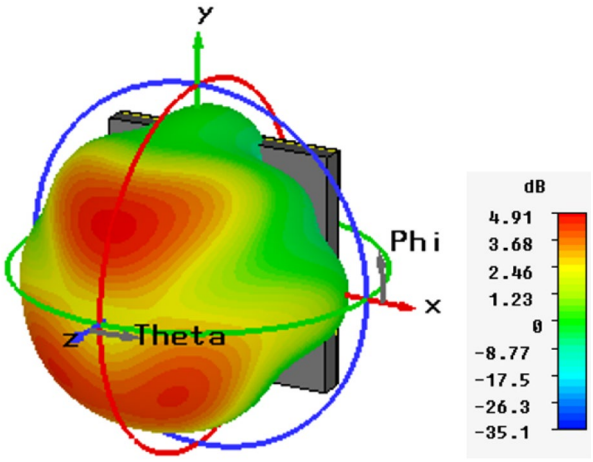

(b)

Fig. 2 The proposed antenna's characteristics; **a** reflection coefficient response and **b** 3D radiation plot

which has a relative permittivity of 2.2. The overall dimensions of the structure are $16 \times 8 \times 0.8$ mm^3, with specific dimensions listed in Table 1 for reference.

As shown in Fig. 5, the simulated S-parameters of the array indicate an impedance bandwidth ranging from 37.6 to 40.8 GHz. The array also exhibits excellent isolation, with a value better than 22 dB across this frequency range, ensuring minimal interference between the radiating elements. This design approach, coupled with careful substrate selection and element spacing, contributes to the array's robust performance in terms of bandwidth and isolation, making it well-suited for high-frequency applications.

Table 1 Dimension of the proposed radiating element

Parameter	Dimension (mm)	Parameter	Dimension (mm)
Ws	8	Ws_2	32
Ls	8	Ls_2	8
Wg	8	Wg_2	32
Lg	8	Lg_2	8
Lf	2	Ws_3	70
Wf	1	Ls_3	16
R	2.5	Wg_3	70
Ra	1	Lg_3	16
Ws_1	16	D	16
Ls1	8		

2.4 Four Element Antenna Array

The geometry of the four-element antenna array is depicted in Fig. 6. The antennas are arranged horizontally on the substrate, with the spacing between adjacent elements carefully optimized to minimize electromagnetic coupling. This design ensures minimal interaction between neighboring antennas, improving overall performance. As shown in Fig. 7, the isolation between individual elements is greater than 25 dB across the entire operational bandwidth, which spans 2.6 GHz, ranging from 37.7 to 40.3 GHz. Additionally, the reflection coefficient remains better than − 10 dB throughout this frequency range, indicating excellent impedance matching. The total footprint of the antenna array is compact, measuring 8×32 mm^2.

2.5 Eight Element Antenna Array

Figure 8 shows the layout of the eight-element antenna array. The radiating elements in the array are strategically arranged such that the radiating elements are arranged on opposite sides on the substrate surface and interleaved to significantly reduce mutual coupling between adjacent elements without the use of a decoupling structure. The array was designed to be 16×70 mm^2 to comply with the form factor constraints typical of modern 5G communication devices. This size enables practical integration into mobile devices while maintaining optimal performance within the target frequency range of 37.7 to 41.3 GHz. We aimed to strike a balance between a compact design and sufficient element spacing, minimizing mutual coupling and optimizing radiation efficiency. Although different sizes could influence performance, simulations and iterative design processes helped us select these dimensions to meet both size and performance requirements. Further size adjustments could affect parameters such as gain, beamwidth, and isolation, but this configuration offers a suitable compromise for the intended application.

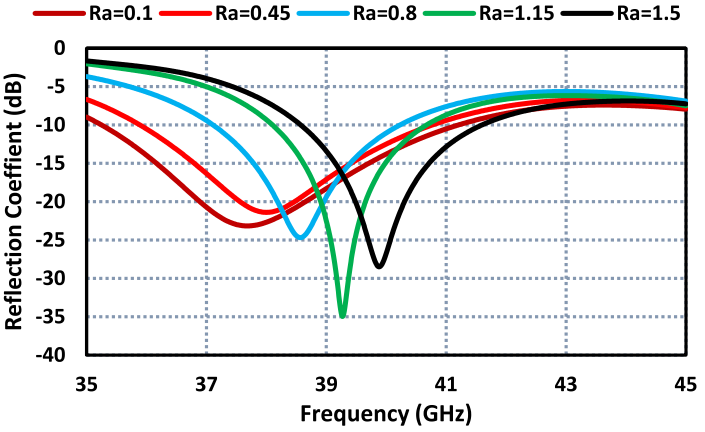

(a)

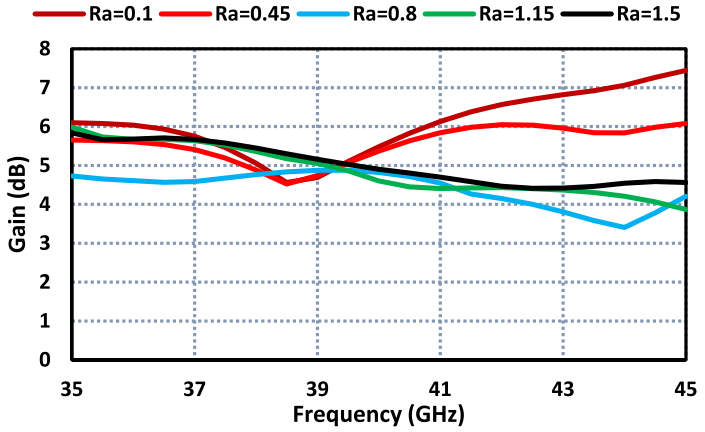

(b)

Fig. 3 Effect of the semi-circular radius (R_a) cut on the circular patch; **a** reflection coefficient response and **b** antenna gain. Dimension of R_a is in millimeters

Table 2 The effect of radius sections (Ra) on the impedance bandwidth and antenna gain performance

Value of R_a (mm)	Freq. range (GHz)	Impedance bandwidth (GHz)	Antenna gain (dB)
0.10	35–41	6	6
0.45	36–41	5	5.8
0.80	37–40	3	5
1.00	37.3–41.3	2.6	4.91
1.15	38–40	2	5
1.50	38.6–41.6	3	5

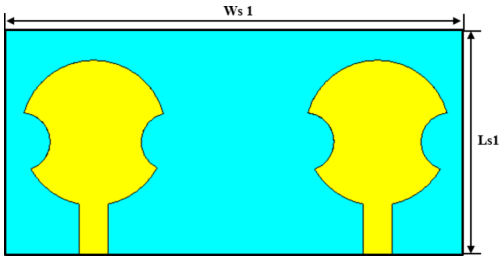

Fig. 4 Two-element antenna array based on the proposed radiating element. Yellow shading represents metallization and blue shading the diectric substrate

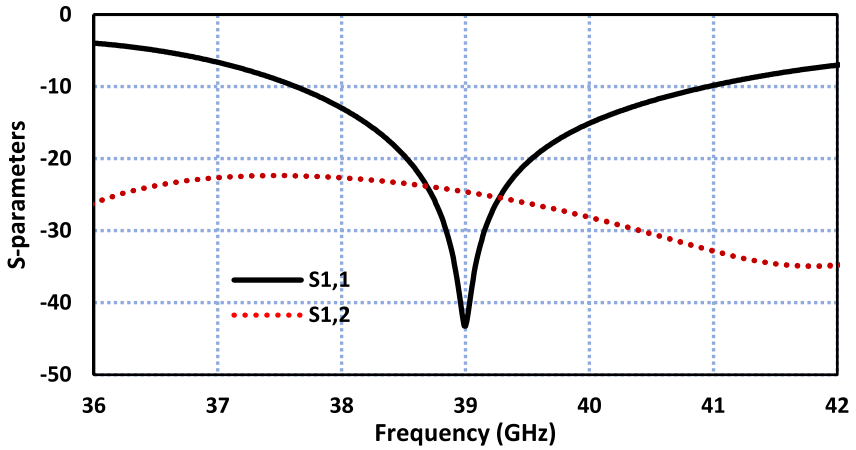

Fig. 5 S-parameters of the two-element antenna array based on the proposed radiating element

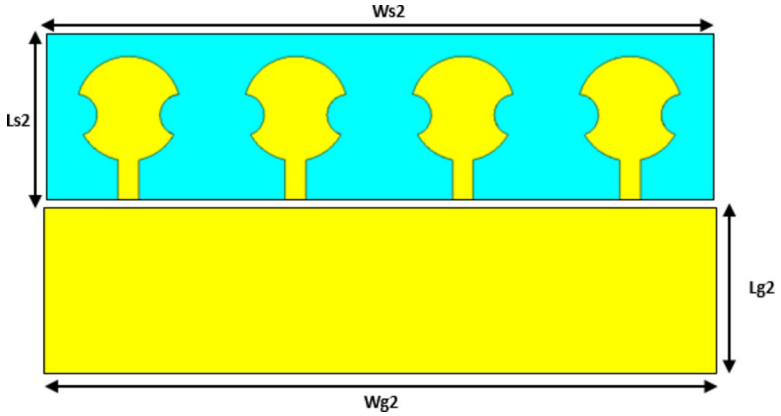

Fig. 6 Proposed 4-element antenna array showing the front and back views. Yellow shading represents metallization and blue shading the diectric substrate

Figure 9 shows the S-parameters of the proposed antenna array, providing insight into its performance. The impedance bandwidth of the array extends from 37.7 to 40.3 GHz, which covers the desired frequency range for the intended 5G

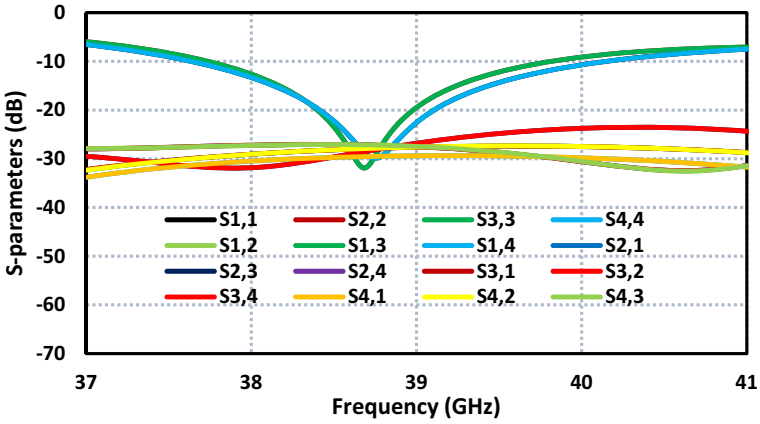

Fig. 7 S-parameters of 4-element antenna array

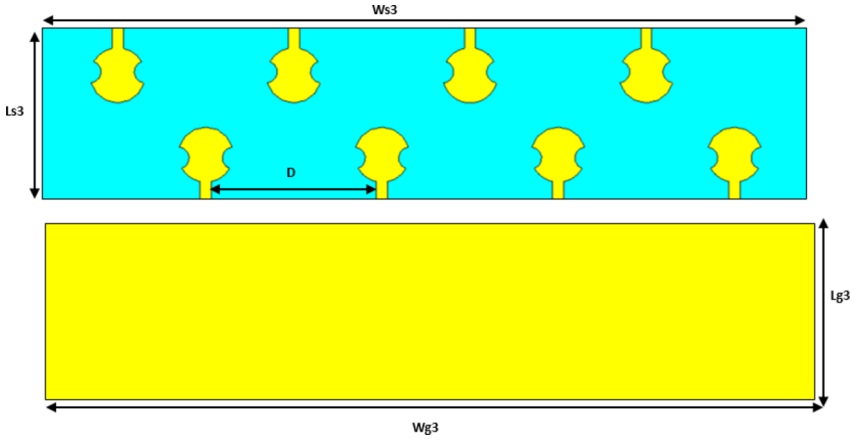

Fig. 8 Proposed 8-element MIMO structure; front view and back view

applications. Within this range, the transmission coefficient remains below – 26 dB, signifying excellent isolation between the radiating elements of the array. This low transmission coefficient is crucial as it minimizes mutual coupling between elements, which could otherwise degrade overall array performance. The strong isolation helps maintain optimal radiation patterns and improves the efficiency of the array by reducing interference between elements. This performance was achieved through careful design and optimization of the element spacing and configuration, ensuring the array meets the stringent requirements of modern communication systems.

Figure 10 shows the radiation patterns of the single-element, 4-element, and 8-element antenna arrays. The half-power beamwidth (HPBW) of the single-element antenna is 120° in the E-plane and 180° in the H-plane. For the 4-element antenna

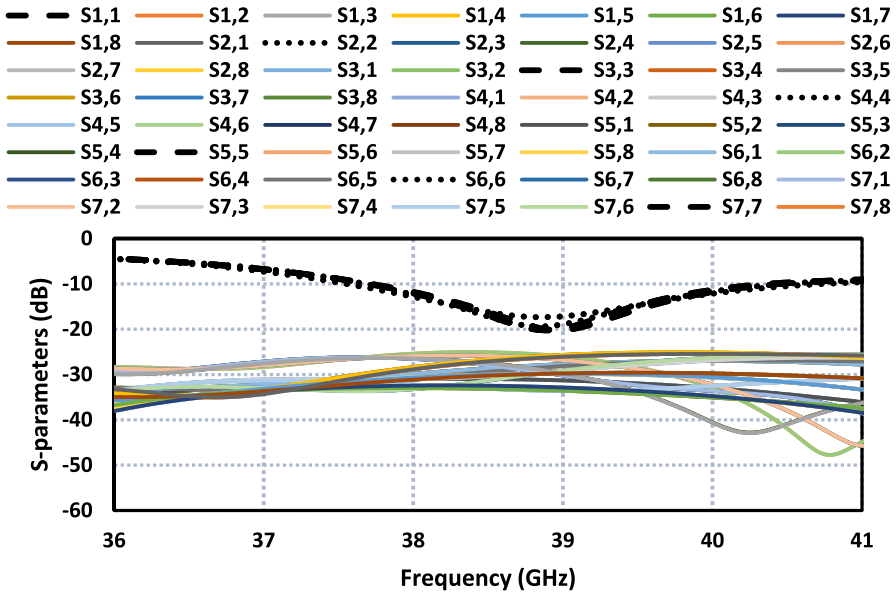

Fig. 9 S-parameters of 8-element antenna array

array, the HPBW in both the E-plane and H-plane is 140°. In contrast, the 8-element antenna array has a HPBW of 90° in the E-plane and 160° in the H-plane.

3 Measured Results

The front and back sides of the fabricated eight-element antenna array are shown in Fig. 11. The array's performance was measured in an anechoic chamber using a Vector Network Analyzer (VNA). The gain was measured using the standard method with a reference horn antenna. The gain of the antenna array was calculated by comparing its received signal strength to that of the reference antenna using the Friis transmission equation:

$$G_{AUT} = G_{ref} + 10log\left(P_{ref}/P_{AUT}\right) \tag{2}$$

where G_{AUT} is the gain of the antenna under test, G_{ref} is the gain of the reference antenna, and P_{AUT} and P_{ref} are the power levels received from the test and reference antennas, respectively.

The radiation pattern measurements were conducted in an anechoic chamber. Additionally, we accounted for signal losses, calibration errors, impedance mismatches between the antenna and the test equipment, positioning errors, and other minor factors using a reference antenna and calibration procedures.

The measured S-parameters of the array are shown in Fig. 12. The results show good agreement between the simulation and measurement. Figure 12b shows that

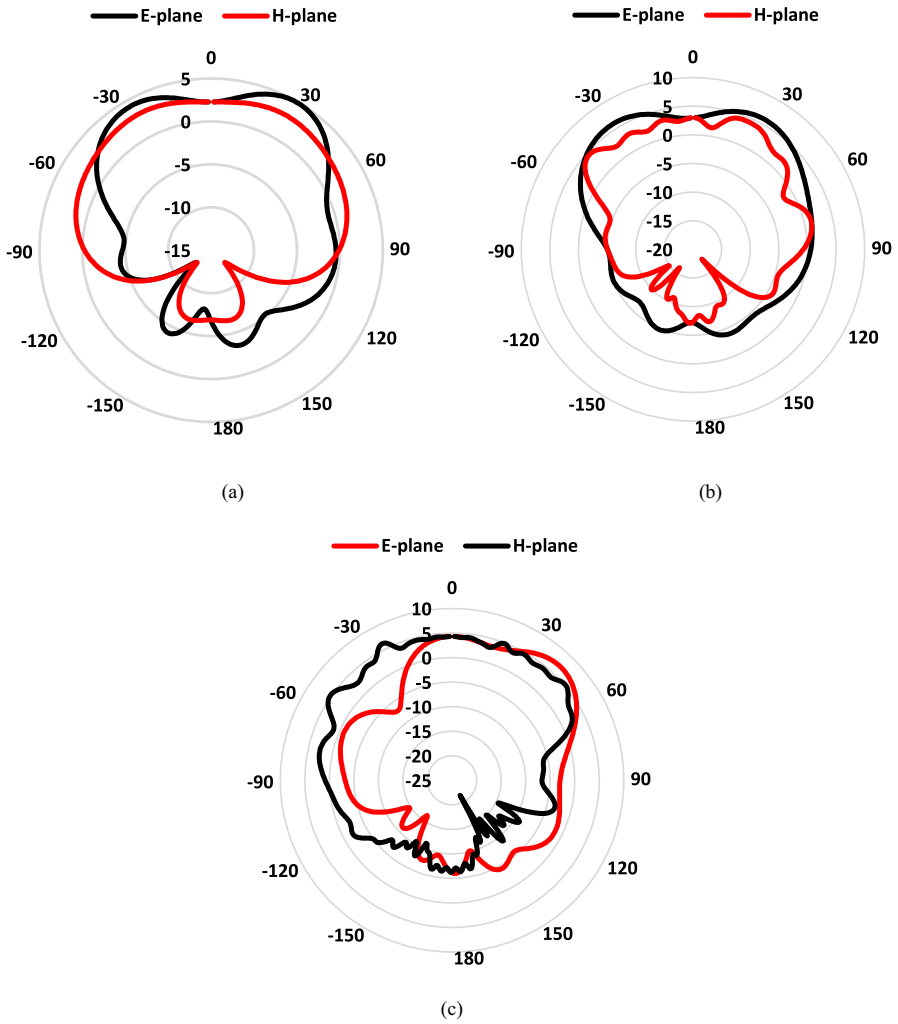

Fig. 10 Simulated radiation pattern at 39 GHz; **a** single-element antenna, **b** 4-element MIMO antenna, and **c** 8-element antenna array

the measured mutual coupling between the various ports (S12, S13, S14, S31, S32, etc.) is better than − 25 dB across the 37.7–40.5 GHz band. This low level of coupling minimizes interference between the ports, which is crucial for achieving high isolation, better radiation patterns, and thereby ensuring reliable 5G communication across the specified frequency range.

Figure 13a presents the simulated and measured 2D radiation patterns of the 8-element antenna array at 39 GHz in the E- and H-planes. The measured results indicate that the array radiates energy omnidirectionally in both planes. Figure 13b shows that the worst-case cross-polarization is limited to 4 dB. Figure 13c, d displays the measured radiation patterns of the array. Figure 14 illustrates the simulated

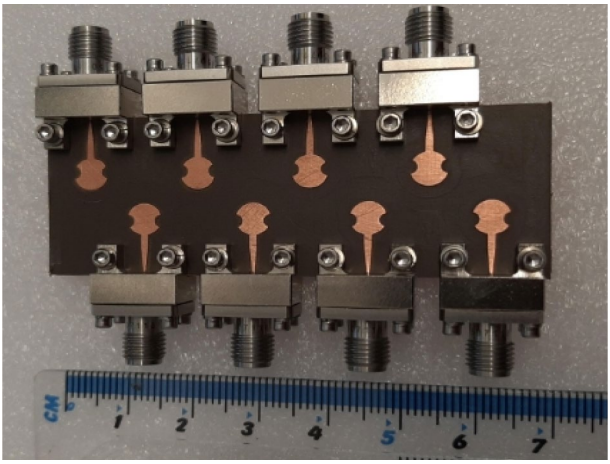

(a)

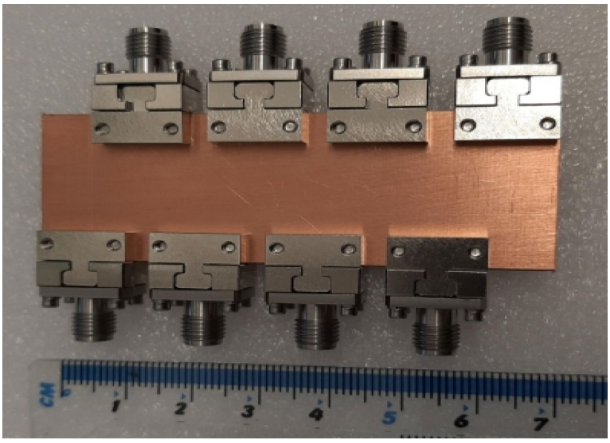

(b)

Fig. 11 Fabricated prototype of the 8-element antenna array; **a** front view and **b** back view

and measured gain performance of the 8-element array. The measured gain ranges from 7.4 to 6 dBi between 37 and 41 GHz.

4 Surface Current Distribution

Figure 15a shows the surface current distribution over the eight-element antenna array at 39 GHz. When only antenna #1 is excited, the current is primarily concentrated around the edges of the antenna and near the feed line close to the radiator. The current distribution has minimal effect on the other radiating elements in the array. Figure 15b illustrates the current distribution when only antenna #4 is excited, while Fig. 15c, d depicts the current distributions when antennas #6 and #8, located

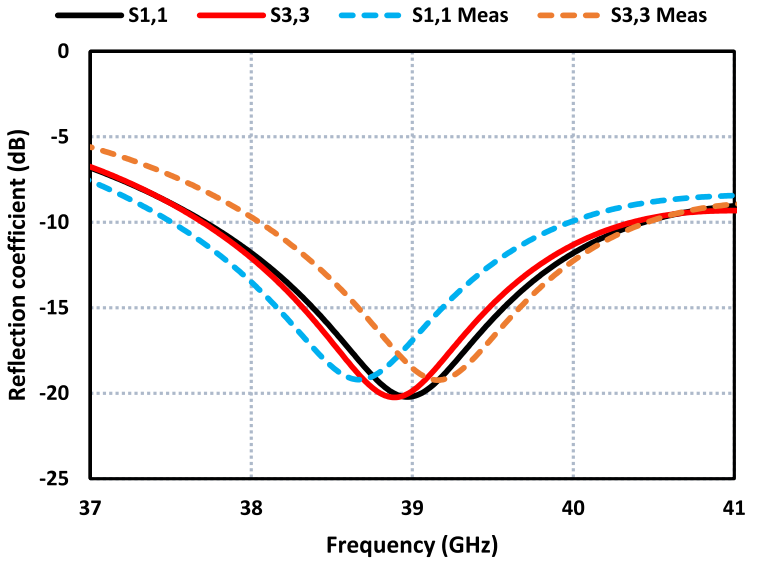

(a)

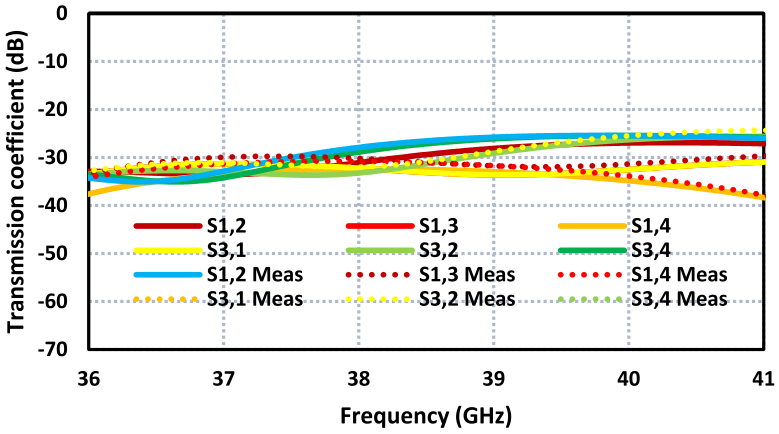

(b)

Fig. 12 S-parameters of 8-element antenna array; **a** reflection coefficient response and **b** transmission coefficient response

on the opposite sides of the array, are individually activated. In all cases, similar current distribution patterns are observed, indicating that the excitation of any specific antenna has virtually no impact on the others.

These results demonstrate that the surface current on any given antenna in the array exhibits minimal interaction with neighboring antennas, which effectively limits mutual coupling between the elements. This low level of mutual coupling is achieved without the need for additional decoupling structures, which simplifies the design and enhances overall performance.

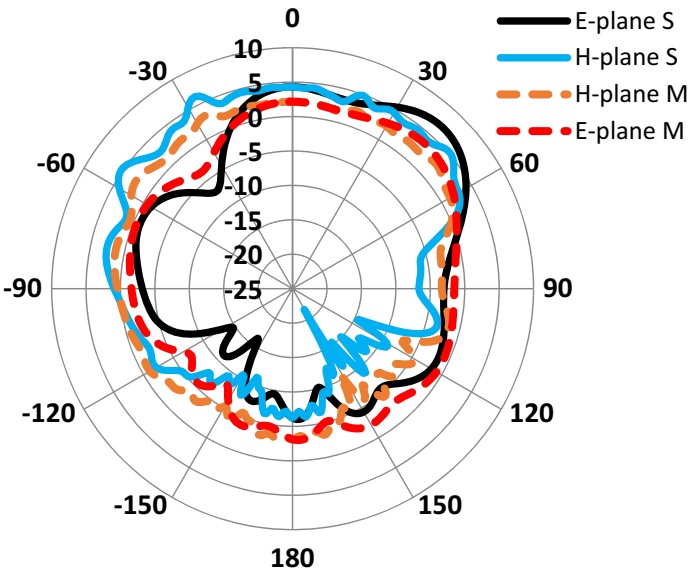

(a)

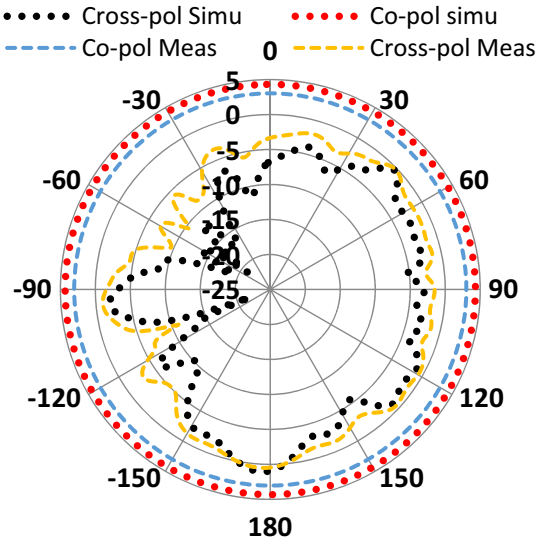

(b)

Fig. 13 Simulated (S) and measured (M) results of the 8-element antenna array; **a** E- and H-planes, **b** co- and cross-polarization, **c** E-plane radiation pattern, and **d** H-plane radiation pattern

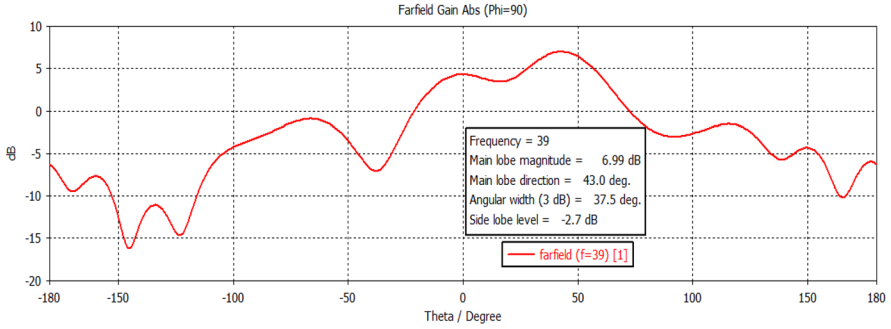

(c)

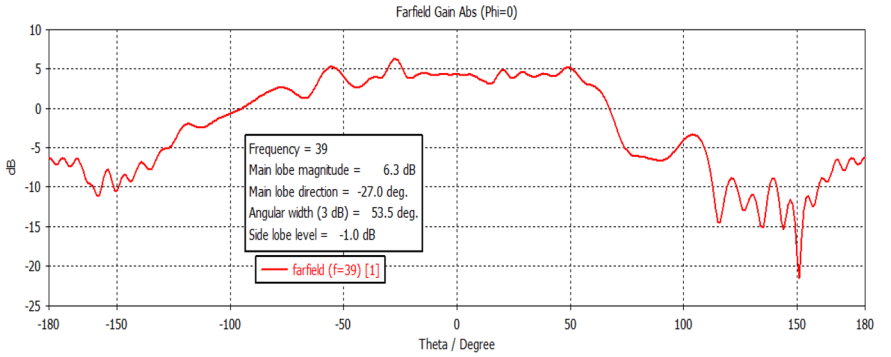

(d)

Fig. 13 (continued)

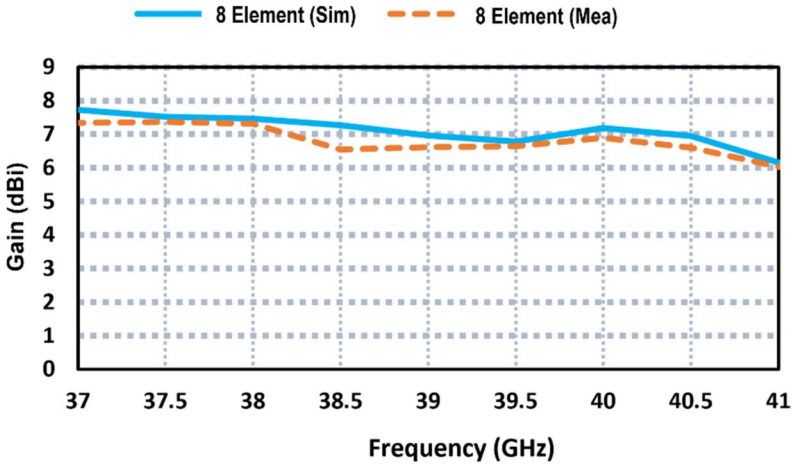

Fig. 14 Simulated and measured gain performance of the proposed 8-element antenna array for MIMO application

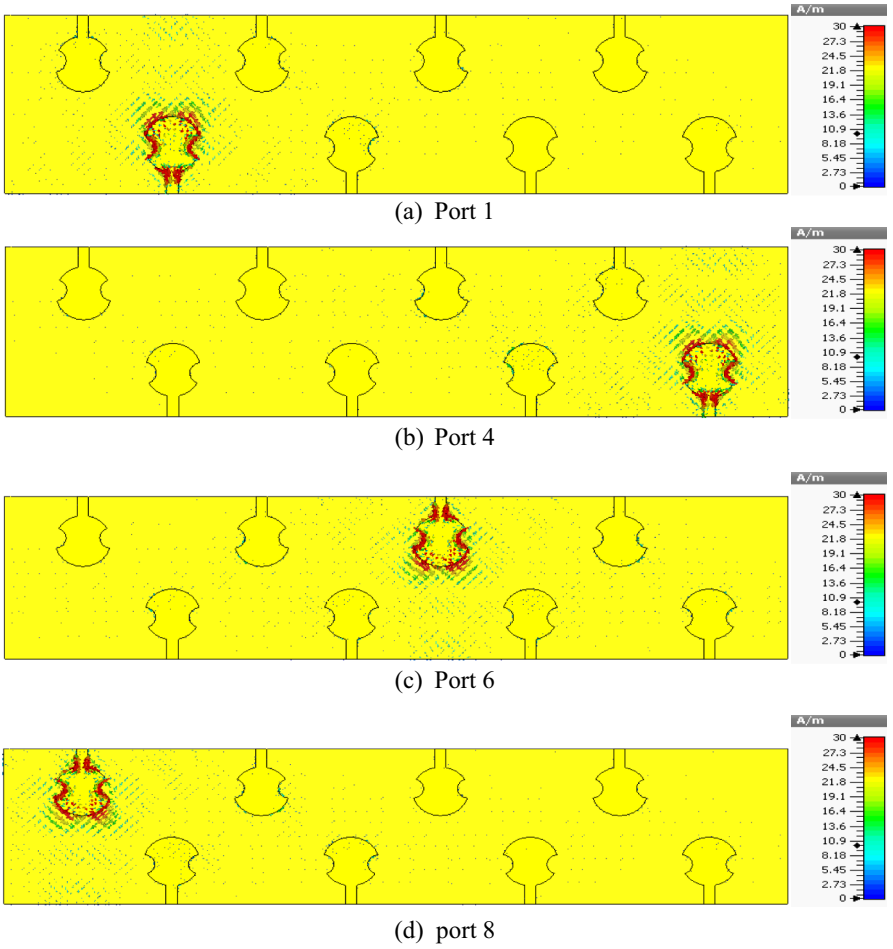

(a) Port 1

(b) Port 4

(c) Port 6

(d) port 8

Fig. 15 Surface current density distribution over the proposed 8-element antenna array at 4.5 GHz; **a** port 1 excitation, **b** port 4 excitation, **c** port 6 excitation, and **d** port 8 excitation

5 MIMO Performance Parameters

5.1 Envelope Correlation Coefficient (ECC)

The degree of mutual coupling between MIMO elements is measured by the Envelope Correlation Coefficient (ECC). In order to reduce coupling effects between the radiating parts, the ECC is required to stay below 0.5. Equation (3) can be used to calculate the ECC [25].

$$ECC = \frac{|\iint 4\pi(M_i)(\theta,\phi)) \times (M_j(\theta,\phi))d\Omega|^2}{\iint 4\pi|(M_i(\theta,\phi))|^2 d\Omega \iint 4\pi|(M_j(\theta,\phi))|^2 d\Omega} \quad (3)$$

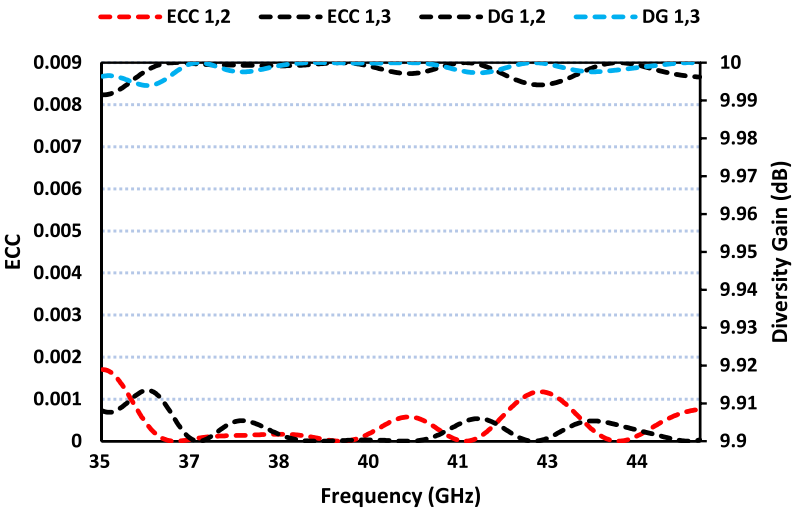

Fig. 16 ECC and DG of proposed 8-element antenna array for MIMO systems

The given equation represents the radiation patterns when ports i and j are excited, with Ω representing the solid angle. Figure 16 shows that the eight-element array for MIMO applications exhibits a low ECC, showing strong isolation between radiating elements.

5.2 Diversity Gain (DG)

Another crucial parameter for assessing MIMO performance is Diversity Gain (DG), which indicates the transmission power losses that occur when diversity patterns are applied to MIMO structures. Equation (4) can be used to estimate the diversity benefit from ECC. Figure 16 shows that the DG of the array is better than 9.99 dB.

$$DG = 10 \times \sqrt{(1 - ECC)} \tag{4}$$

6 Comparison with the Work Reported in Literature

The proposed 8-element antenna array is designed for the 5G wireless communication band, operating between 37.7 and 41.3 GHz, as specified in the USA and Canada. The antenna is compared with other antenna arrays in Table 3. Most antennas reported in the literature generally focus on the 28 GHz band. With 8 ports, the array offers greater diversity and flexibility compared to the commonly reported 2- or 4-port designs. The array's compact dimensions ($16 \times 70 \times 0.8$ mm^3) make it competitive in terms of size, especially compared to larger designs.

In terms of isolation, the array achieves more than 25 dB, which is comparable to many other works, though slightly lower than the extreme isolation of 64 dB

Table 3 Comparison with the work reported in literature

Ref	f_r (GHz)	Ports	Dimension (mm)	Isolation (dB)	Diversity gain (dB)	ECC	Technique
[18]	28	2	30×15×0.25	35.8	5.42	<0.005	DGS
[19]	27	4	30×30×1.575	30	7.1	0.0005	DGS
[20]	28	4	30×35×0.76	17	8.3	<0.01	DGS
[21]	28	2	15×25×0.203	30	5.8	<0.005	DGS
[22]	28	4	30×30×0.787	29	6.1	<0.16	DGS
[23]	28	4	20×40×1.6	29.34	7	<0.01	DRA
[24]	27	4	30×28×0.508	24	6.22	<0.05	DGS
[25]	28	2	18×38×0.8	64	8.75	<0.005	DGS
[26]	3.2–14	1	62.5×62.5×25	-	8.1	-	DGS
[27]	3–15	1	62.5×62.5×25	-	8.1	-	DGS
[29]	38	1×16	90.49×29.43	-	16.4	-	-
[30]	28	1	58.86×69.45	-	8.64	-	FGS
[31]	27	4	28×30	>22	6.2	0.05	DGS
[32]	35	4	12.5×12.5	>21	6	0.02	DGS
[33]	28.5	4	115×65	>12	4.85	0.1	DGS
[34]	28	4	36×28×0.8	>30	-	0.005	DGS
This work	37.7–40.3	8	16×70×0.8	>25	7.5	<0.005	Full ground plane

reported in some designs. The diversity gain of the proposed array is 7.5 dB, positioning it among the better-performing antennas, although a few designs exhibit slightly higher gains, such as 8.75 dB in reference [25]. Additionally, the array demonstrates an extremely low envelope correlation coefficient (ECC) of less than 0.005, which matches the best performance reported in the literature, ensuring minimal interference between ports.

Unlike most designs that rely on techniques such as Decoupling Ground Structures (DGS) or Dielectric Resonator Antennas (DRA) to reduce mutual coupling, the proposed array uses a full ground plane. This approach simplifies the design without compromising its performance, making it a robust and efficient option for integration into modern 5G communication systems. Overall, the proposed antenna array offers a well-balanced combination of compact size, high isolation, excellent diversity gain, and low ECC, making it a strong competitor against other designs reported in the literature.

7 Conclusion

This article introduced an innovative eight-element antenna array designed for MIMO systems, operating across a broad frequency range of 37.7 to 40.3 GHz, which is ideal for 5G mm-wave applications. The array features a strategic arrangement of radiating elements, with elements positioned on opposite sides of the

substrate surface and interleaved to effectively minimize mutual coupling between adjacent antennas. Mutual coupling, the interference caused by closely spaced antennas, can negatively impact performance by introducing unwanted interactions and reducing signal quality. The interleaved arrangement and opposite-side positioning of the radiating elements significantly mitigate these coupling effects.

The proposed antenna array demonstrates impressive performance metrics. The isolation between radiating elements exceeds 25 dB across the operational frequency range, which ensures minimal interference between elements. The array achieves a maximum gain of 7.5 dB and an overall efficiency of 80%, with an impedance bandwidth of 2.6 GHz. Additionally, the antenna array exhibits excellent Envelope Correlation Coefficient (ECC) and diversity gain performance, contributing to its robustness and reliability.

However, practical deployment of such high-frequency systems faces challenges, including signal attenuation, limited range due to the nature of millimeter waves, and susceptibility to blockage by physical obstacles. To address these issues, solutions such as advanced beamforming techniques, sophisticated signal processing, and optimal placement of antenna arrays are proposed. These strategies aim to enhance system performance and mitigate the inherent challenges of operating in millimeter-wave frequencies.

Author Contribution Conceptualization, N.A.A., B.V., I.U.D., S.U., A.A.A., N.R., M.S., C.H.S., M.A.,; methodology, N.A.A., B.V., I.U.D., M.S., M.A.,; software, N.A.A., B.V., I.U.D.; validation, N.A.A., B.V., I.U.D., S.U., A.A.A., N.R., M.S., C.H.S., M.A.; formal analysis, N.A.A., B.V., I.U.D., M.S., M.A.; investigation, B.V., S.U., A.A.A., N.R., M.S., M.A.; resources, N.A.A., B.V., I.U.D., C.H.S., M.A.; data curation, N.A.A., B.V., I.U.D., S.U., N.R., C.H.S., M.A.; writing—original draft preparation, N.A.A., B.V., I.U.D., M.A.; writing—review and editing, N.A.A., B.V., I.U.D., S.U., A.A.A., N.R., M.S., C.H.S., M.A.; visualization, N.A.A., B.V., I.U.D., S.U., A.A.A., N.R., M.S., C.H.S., M.A.; supervision, M.A.; project administration, M.A.; funding acquisition, M.A.. All authors have read and agreed to the published version of the manuscript.

Data Availability No datasets were generated or analysed during the current study.

Declarations

Competing Interests The authors declare no competing interests.

Disclaimer All of the figures, materials, and data within the manuscript are original and owned by the authors.

References

1. Lien, S.-Y.; Shieh, S.-L.; Huang, Y.; Su, B.; Hsu, Y.-L.; Wei, H.-Y. 5G new radio: Waveform, frame structure, multiple access, and initial access. IEEE Commun. Mag. 2017, 55, 64-71.
2. Javaid, N.; Sher, A.; Nasir, H.; Guizani, N. Intelligence in IoT-based 5G networks: Opportunities and challenges. IEEE Commun. Mag. 2018, 56, 94-100.
3. Li, A.; Luk, K.-M. Single-layer wideband end-fire dual-polarized antenna array for device-to-device communication in 5G wireless systems. IEEE Trans. Veh. Technol. 2020, 69, 5142-5150.
4. Ullah, R.; Ullah, S.; Ullah, R.; Din, I.U.; Kamal, B.; Khan, M.A.H.; Matekovits, L. Wideband and High Gain Array Antenna for 5G Smart Phone Applications Using Frequency Selective Surface. IEEE Access 2022, 10, 86117-86126.
5. Hong, W.; Jiang, Z. H.; Yu, C.; Hou, D.; Wang, H.; Guo, C.; Kuai, Y. L. H.; Yu, Y.; Jiang, Z.; Chen, Z.; Chen, J.; Yu, Z.; Zhai, J.; Zhang, N.; Tian, L.; Wu, F.; Yang, G.; Hao, Z.-C.; Zhou, J. Y. The role of millimeter-wave technologies in 5G/6G wireless communications. IEEE J. Microw. 2021, 1 (1), 101-122.
6. Rodriguez-Cano, R.; Zhao, K.; Zhang, S.; Pedersen, G. F. "Handset frame blockage reduction of 5G mm-Wave phased arrays using hard surface inspired structure." IEEE Trans. Veh. Technol. 2020, 69(8), 8132–8139.
7. Ozpinar, H.; Aksimsek, S.; Tokan, N. T. "A novel compact, broadband, high gain millimeter-wave antenna for 5G beam steering applications." IEEE Trans. Veh. Technol. 2020, 69(3), 2389–2397.
8. Sulyman, A. I.; Nassar, A. T.; Samimi, M. K.; Maccartney, G. R.; Rappaport, T. S.; Alsanie, A. "Radio propagation path loss models for 5G cellular networks in the 28 GHZ and 38 GHZ millimeter-wave bands." IEEE Commun. Mag. 2014, 52(9), 78–86.
9. Hong, W.; Baek, K.-H.; Ko, S. "Millimeter-wave 5G antennas for smartphones: Overview and experimental demonstration." IEEE Trans. Antennas Propag. 2017, 65(12), 6250–6261.
10. Guo, J.; Liao, S.; Xue, Q.; Xiao, S. "Planar aperture antenna with high gain and high aperture efficiency for 60-GHz applications." IEEE Trans. Antennas Propag. 2017, 65(12), 6262–6273.
11. Dahri, M. H.; Janaluddin, M. H.; Khalily, M.; Abbasi, M. I.; Selvaraju, R.; Kamarudin, M. R. "Polarization diversity and adaptive beamsteering for 5G reflectarrays: A Review." IEEE Access 2018, 6, 19451–19464.
12. Chen, I-J.; Huang, C.-S.; Hsu, P. "Circularly polarized patch antenna array fed by coplanar waveguide." IEEE Trans. Antennas Propag. 2004, 52(6), 1607–1609.
13. Yuan, T.; Yuan, N.; Li, L.-W. "A novel series-fed taper antenna array design." IEEE Antennas Wireless Propag. Lett. 2008, 7, 362–365.
14. Bilgic, M. M.; Yegin, K. "Wideband offset slot-coupled patch antenna array for X/Ku-band multimode radars." IEEE Antennas Wireless Propag. Lett. 2014, 13, 157–160.
15. Ye, S.; Geng, J. P.; Liang, X. L.; Guo, Y. J.; Jin, R. H. "A compact dual-band orthogonal circularly polarized antenna array with disparate elements." IEEE Trans. Antennas Propag. 2015, 63(4), 1359–1364.
16. Biswas, A. K.; Chakraborty, U. "Reduced mutual coupling of compact MIMO antenna designed for WLAN and WiMAX applications." Int J RF Microw Comp-Aid Eng. 2019, 29(3), e21629.
17. Biswal, S. P.; Das, S. "A planar triple band four element antenna system with polarization and pattern diversity for LTE/WLAN/DSRC applications." Int J RF Microw Comput-Aid Eng. 2018, 28(4), e21213.
18. Hussain, N.; Awan, W. A.; Ali, W.; Naqvi, S. I.; Zaidi, A.; Le, T. T. "Compact wideband patch antenna and its MIMO configuration for 28 GHz applications." AEU-International Journal of Electronics and Communications 2021, 132, 153612.
19. Hussain, M.; Mousa Ali, E.; Jarchavi, S. M. R.; Zaidi, A.; Najam, A. I.; Alotaibi, A. A.; Althobaiti, A.; Ghoneim, S. S. "Design and Characterization of Compact Broadband Antenna and Its MIMO Configuration for 28 GHz 5G Applications." Electronics 2022, 11(4), 523.
20. Khalid, M.; Naqvi, S. I.; Hussain, N.; Rahman, M.; Mirjavadi, S. S.; Khan, M. J.; Amin, Y. "4-Port MIMO antenna with defected ground structure for 5G millimeter wave applications." Electronics 2020, 9(1), 71.
21. Zahra, H.; Awan, W. A.; Ali, W. A. E.; Hussain, N.; Abbas, S. M.; Mukhopadhyay, S. "A 28 GHz broadband helical inspired end-fire antenna and its MIMO configuration for 5G pattern diversity applications." Electronics 2021, 10(4), 405.

22. Kamal, M. M.; Yang, S.; Ren, X. C.; Altaf, A.; Kiani, S. H.; Anjum, M. R.; Iqbal, A.; Asif, M.; Saeed, S. I. "Infinity shell shaped MIMO antenna array for mm-wave 5G applications." Electronics 2021, 10(2), 165.
23. Murthy, N. "Improved isolation metamaterial inspired mm-Wave MIMO dielectric resonator antenna for 5G application." Progress in Electromagnetics Research C 2020, 100, 247-261.
24. Khalid, H.; Khalid, M.; Fatima, A.; Khalid, N. "2×2 MIMO antenna with defected ground structure for mm-wave 5G applications." In 2019 13th International Conference on Mathematics, Actuarial Science, Computer Science and Statistics (MACS), 2019, 1–6.
25. Din, I. U.; Ullah, S.; Mufti, N.; Ullah, R.; Kamal, B.; Ullah, R. "Metamaterial-based highly isolated MIMO antenna system for 5G smartphone application." International Journal of Communication Systems 2023, e5392.
26. Din, I. U.; Ullah, S.; Naqvi, S. I.; Ullah, R.; Ullah, S.; Ali, E. M.; Alibakhshikenari, M. "Improvement in the Gain of UWB Antenna for GPR Applications by Using Frequency-Selective Surface." International Journal of Antennas and Propagation 2022.
27. Din, I. U.; et al. "A Novel Compact Ultra-Wideband Frequency-Selective Surface-Based Antenna for Gain Enhancement Applications." Journal of Electromagnetic Engineering and Science 2023, 23(2), 108–121.
28. Din, I.; Ullah, S.; Ullah, K.; Fawad, Y.; Ahmad, I.; Ullah, S.; Habib, U. "Circular monopole ultra-wideband (UWB) antenna with reconfigurable band-notched characteristics." IEEE 23rd International Multitopic Conference (INMIC), 2020, 1–6.
29. H. U. Tahseen, Z. Zheng, and L. Yang, "A Single Substrate 38 GHz Dual Antenna Array with Compact Feed Network," IEEJ Transactions on Electrical and Electronic Engineering, vol. 16, no. 9, pp. 1203-1208, 2021.
30. H. U. Tahseen, L. Yang, and W. Hongjin, "A Broadband H-plane Printed Horn Antenna with Sandwich Substrate Structure for Millimeter-wave Applications," The Applied Computational Electromagnetics Society Journal (ACES), pp. 295–301, 2021.
31. H. Khalid, M. Khalid, A. Fatima, and N. Khalid, "2 × 2 MIMO antenna with defected ground structure for mm-wave 5G applications," in Proc. 2019 13th Int. Conf. Mathematics, Actuarial Science, Computer Science and Statistics (MACS), Karachi, Pakistan, Dec. 14–15, 2019, pp. 1–6.
32. H. Xing, X. Wang, Z. Gao, X. An, H. Zheng, M. Wang, and E. Li, "Efficient Isolation of an MIMO Antenna Using Defected Ground Structure," Electronics, vol. 9, no. 1265, 2020.
33. M. Ikram, M. S. Sharawi, and A. Shamim, "A novel very wideband integrated antenna system for 4G and 5G mm-wave applications," Microwave and Optical Technology Letters, vol. 59, no. 12, pp. 3082-3088, Dec .2017.
34. I. u. D. Din, N. A. Abbasi, W. Ullah, S. Ullah, M. A. Ouameur, and D. N. K. Jayakody, "A Novel and Compact Metamaterial-Based Four-Element MIMO Antenna System for Millimeter-Wave Wireless Applications with Enhanced Isolation, ," Int. J. Antennas Propag., vol. 2024, no. 1, pp.

Authors and Affiliations

Nisar Ahmad Abbasi[1] · Bal Virdee[2] · Iftikhar Ud Din[3] · Sadiq Ullah[3] · Ayman A. Althuwayb[4] · Nasr Rashid[4,5] · Mohammad Soruri[6] · Chan Hwang See[7] · Mohammad Alibakhshikenari[8]

✉ Chan Hwang See
c.see@napier.ac.uk

✉ Mohammad Alibakhshikenari
alibakhshikenari@ing.uniroma2.it

Nisar Ahmad Abbasi
nisar@uhb.edu.sa

Bal Virdee
b.virdee@londonmet.ac.uk

Iftikhar Ud Din
iftikharuddin114@gmail.com

Sadiq Ullah
sadiqullah@uetmardan.edu.pk

Ayman A. Althuwayb
aaalthuwayb@ju.edu.sa

Nasr Rashid
nasrrashid34.el@azhar.edu.eg

Mohammad Soruri
mohamad.soruri@birjand.ac.ir

[1] Department of Electrical Engineering, University of Hafr Al Batin, Hafr Al Batin 39524, Saudi Arabia

[2] Center for Communications Technology, London Metropolitan Unversity, 166-220 Holloway Road, London N8 8DB, U.K.

[3] Telecommunication Engineering Department, University of Engineering and Technology, Mardan 23200, Pakistan

[4] Electrical Engineering Department, College of Engineering, Jouf University, Sakaka, Aljouf 72388, Saudi Arabia

[5] Department of Electrical Engineering, Faculty of Engineering, Al-Azhar University, Nasr City, Cairo 11884, Egypt

[6] Faculty of Ferdows Technical, University of Birjand, Birjand, Iran

[7] School of Computing, Engineering and the Built Environment, Edinburgh Napier University, 10 Colinton Rd, Edinburgh EH10 5DT, U.K.

[8] Electronics Engineering Department, University of Rome “Tor Vergata”, 00133 Rome, Italy